Radiation Hardness of *n*-type SiC Schottky Barrier Diodes Irradiated with MeV He Ion Microbeam

Željko Pastuović[1], Ivana Capan[2], David D. Cohen[1], Jacopo Forneris[3], Naoya Iwamoto[4], Takeshi Ohshima[4], Rainer Siegele[1], Norihiro Hoshino[5], Hidekazu Tsuchida[5],

[1]*Australian Nuclear Science and Technology Organisation, Locked bag 2001, Kirrawee DC NSW 2232, Australia*

[2] *Material Physics division, Institute Rudjer Boskovic, POBox 180, 10000 Zagreb, Croatia*

[3] *Physics Department and NIS Excellence Centre, University of Torino, via P. Giuria 1, 10125 Torino, Italy*

[4] *Japan Atomic Energy Agency, 1233 Watanuki, Takasaki, Gunma 370-1292, Japan*

[5] *Central Research Institute of Electric Power Industry, 2-6-1 Nagasaka, Yokosuka, Kanagawa 240–0196, Japan*

The radiation hardness of 4H-SiC Schottky barrier diodes (SBD) for the light ion detection and spectroscopy in harsh radiation environments is tested and compared with recent results obtained by *n*-type silicon diodes. *n*-type SBD prepared on an epitaxial grown 4H-SiC thin wafers have been irradiated by a raster scanned alpha particle microbeam (2 & 4 MeV He^{2+} ions separately) in order to create patterned damage structures at different depths within a sensitive volume of tested diodes. Deep level transient spectroscopy (DLTS) analysis revealed formation of two deep electron traps in the irradiated and not thermally treated 4H- SiC that resemble those already reported in the literature, the S_1 and $Z_{1/2}$ defects. Ion Beam Induced Charge (IBIC) microscopy with multiple He ion probe microbeams (1-6 MeV) having different penetration depths in tested SBD has been used to determine a degradation of the charge collection efficiency over wide fluence range of damaging alpha particle. The non-linear behavior of the CCE decrease and the significant deterioration of spectroscopic performance with increasing He ion fluence was observed above the value of 10^{11} cm^{-2}. Our results test a hypothesis of better radiation hardness of the 4H-SiC compared to silicon materials used for particle (ion) detection applications in MeV energy range.

Keywords: Silicon carbide, CCE, Ion radiation effects, Radiation hardness, Detectors, Deep defects

Corresponding author: Zeljko Pastuovic, zkp@ansto.gov.au

1. Introduction

The deep level defects that act as charge carrier traps have high importance in semiconductor industry and applications of semiconductor devices [1, 2]. These defects are being created during: a) semiconductor growth process, b) electronic device fabrication and c) operation in harsh environments. We focus our attention on defects created in semiconductor devices exposed to irradiation by ions [3, 4, 5, and 8] and electrons [6, 7] in the MeV energy range.

It is well known that high energy ionizing particles traversing through or being stopped in a sensitive volume of semiconductor device, deposit part of their initial energy in atomic elastic collisions displacing them from their lattice sites [9]. Those primary defects might annihilate or reorganize themselves with impurities to form stable deep defects. Defect accumulation in reasonably low concentrations (well below an extended defect formation threshold value) might modify electronic transport properties of charge carriers introduced into active region of a device, and consequently alter or deteriorate its performance [3-8, 10-15].

Silicon carbide is widely regarded as a semiconducting material, which has desirable physical properties (high thermal conductivity, large saturation electron drift velocity, high electric breakdown field, and excellent thermal stability) for manufacturing of electronic devices suitable for applications in harsh environments, i.e. high radiation [13, 14, 16], high temperature [17, 18], and high power applications [19-21]. In this study we investigate the radiation hardness of single crystal 4H-SiC material for particle detection in intense radiation conditions. The radiation hardness of SiC detectors has been studied using irradiation with neutrons [14], protons [11, 12, 13, 16], gamma photons [12], electrons [6, 12, 13], light ions [11] and heavy ions [11, 15].

The 4H-SiC epitaxial growth technique achieving high growth rate and large area crystal uniformity has been developed recently [22]. Utilizing a modified epi-reactor setup, a thickness uniformity of 1.1% and a doping uniformity of 6.7% for a 65-mm-radius area has been achieved, while maintaining a high growth rate of 80 μm/h. Epi-layers of lightly doped 4H-SiC, obtained by this technique, show low concentrations of $Z_{1/2}$ and $EH_{6/7}$ defects and a very good carrier lifetime making it very suitable for electronic applications discussed previously. We used the grown epi-layer to fabricate Schottky barrier diodes (SBD in further text) for ionizing radiation detection and monitoring, and exposed them to a radiation hardness test.

2. Experimental

n-type silicon carbide SBDs were produced on nitrogen-doped (up to 4–5×10^{14} cm^{-3}) epitaxial grown 4H-SiC single crystal layers approximately 47 μm thick [22]. The Schottky barrier was formed by evaporation of nickel through a metal mask with patterned quadratic apertures of 1 mm × 1 mm, while Ohmic contacts were formed by nickel sintering at 950C in Ar atmosphere on the back side of the silicon carbide substrate. The reverse negative bias was connected to the front Schottky contact, and the back Ohmic contact of prepared 4H-SiC SBD was grounded.

The whole testing procedure for this particular 4H-SiC material follows in slightly modified conditions the experimental protocol previously used on silicon diodes [3, 4]. The quality of the 4H-SiC SBDs was characterized by I–V and C–V measurements. Only samples with the lowest reverse current have been considered for our radiation hardness study. Additional care was taken during final sample selection by performing the scanning Ion Beam Induced Charge (IBIC) microscopy [23] in frontal mode (ion microbeam with a very low rate of up to 1000 cps is scanned perpendicular over a front metal contact) on each pre-selected sample to establish a good uniformity of charge collection efficiency (CCE) across the whole active SBD volume. Subsequent irradiation conditions meant to generate defects in 4H-SiC layer have been optimized for a) direct single ion detection and counting utilizing the IBIC technique and b) Deep Level Transient Spectroscopy (DLTS) on irradiated samples.

The selected samples were homogenously irradiated with a 2 MeV He ion microbeam at the ANSTO heavy ion microprobe facility [24]. Details about ion beam rates, irradiation fluences and patterns for tested 4H-SiC SBD samples are given in Table1. All irradiations have been performed at the room temperature and zero bias. The samples have not been thermally treated after irradiations. Negligible error might have been caused by a dead time of the microprobe DAQ system in given working conditions.

For C-V and DLTS measurements the micro–beam with 10000 cps ion rate (~2.5×10^{11} $cm^{-2}s^{-1}$) was raster scanned multiple times over the total irradiated area of approximately 1mm × 1mm in order to avoid an instantaneous implantation of the full dose as well as ion beam supported self-annealing of primary defects, and also achieve a homogenous single ion implantation over extended time. The scan area was divided in 512×512 pixels with a dwell time per pixel equal to 500 or 1000 μs, i.e. on the average up to 5 ions were implanted in each pixel before the micro–beam was moved to the next pixel position. Total time required to

homogenously irradiate SBDs was 33 min (#3), 83 min (#8), 166 min (#4) and 333 min (#12) respectively.

Deep traps created in silicon carbide were characterized using DLTS. DLTS measurements were performed at temperatures between 80 and 380 K. No deep traps have been detected in non-irradiated samples. Eight different rate windows from 0.5 to 100 ms were simultaneously obtained from one temperature scan in order to determine the DLTS signature of formed defects (activation energy and the trap concentration).

Detrimental influence of defects formed in active 4H-SiC epi-layer on the CCE of selectively irradiated SBDs has been investigated by the scanning IBIC microscopy. The amplitude of the IBIC signal was recorded for each ion implanted in nine (3×3) squares of 100×100 μm^2 each with a 100 μm gap between them [3]. Each square was irradiated with increasing fluence value from 10^9 to $5\times10^{11} cm^{-2}$ using optimized microbeam conditions (Table1). Two samples have been pattern irradiated in the same way using 4 MeV He (#1) and 2 MeV He (#2) *damaging ion (micro) beam* (further in text referred as DIB) respectively. After patterned irradiations the different ions probes or *probing ion (micro) beams* (further in text referred as PIB, PIB = 1, 2, 3, 4, and 6 MeV He) and reverse bias settings of -100, -200 and -400 V have been used for IBIC microscopy of partially damaged SBDs to monitor deterioration of the total charge collection. For radiation damage studies we considered only IBIC events originating from a central part of the irradiated square areas 50×50 μm^2 showing uniform IBIC response, with no changes towards edges of irradiated areas. The reported CCE values represent the centroids of the induced charge pulse spectra relevant to each irradiated regions and normalized to the signal resulting from pristine material.

3. Results and discussions

A. Electrical characterization of 4H-SiC SBD

The electrical characterization of a typical pristine 4H-SiC SBD sample suitable for studies is shown in Fig.1. The measured reverse current is below 4 pA over the full reverse bias range (Fig.1a), while the forward current increases sharply above ca. +0.6 V. The low reverse current through SBD is necessary for IBIC measurements, i.e. detection of the current transient induced by motion of free charge carriers (generated by single ions) in a depleted region of tested device. As prepared the 4H-SiC SBDs were able to withstand a reverse bias of up to -450 V maintaining a low reverse current and electronic noise. The measured C-V

characteristic (Fig.1b) was used to calculate the free carrier concentration profile in the region of interest of a pristine SBD (Fig.1c). It was calculated to be of the order of 4-5×10^{14} cm^{-3}. The calculated depletion thickness (*w*) as a function of applied reverse bias is shown in Fig. 1(d). Calculated approximate *w* values for IBIC settings of -100 V, -200 V and -400 V are 13.7 μm, 18.5 μm and 25.1 μm, respectively. The voltage settings required for the DLTS measurements were chosen from the comparison of SRIM [25] simulations for the extent of disordered region dense with primary displacements following the single 2.0 MeV He ion implantation in silicon-carbide (later shown in Fig.5c) and doping profiles of implanted samples calculated from corresponding C–V measurements (Fig.2). The applied reverse bias was varied between -3 and -5 V with a filling pulse of 0.5 V to sample the region of interest in SBDs. The cumulative decrease of the free carrier concentration in the irradiated SBDs across the whole section from surface to the extent of implantation range (Fig.2) is supporting the fact that electron traps are formed within implantation range. A variation of the calculated net free carrier concentration can be simulated with an exponentially decreasing function of damaging ion fluence in the tested range (inset of Fig.2).

B. Trap characterization in He ion irradiated 4H-SiC

Summarized results of DLTS studies performed at temperatures from 80 to 380 K using 4H-SiC SBD samples irradiated with different fluences of raster scanned 2 MeV He ion microbeam are shown in Fig.3. All shown spectra were measured at a reverse bias of -4 V and the rate window of 50ms. Only one electron trap (E1) with its maximum at about 280 K has been observed in the sample irradiated up to fluence of 1×10^{9} cm^{-2} (black curve), while two electron traps (E1 and E2) with their maxima at about 280 and 330 K have been observed in the sample irradiated up to the total fluence of 1×10^{10} cm^{-2} (red curve). Again, one trap with a peak maximum at about 330K (E1) was observed for the highest fluence 2×10^{10} cm^{-2} (blue curve). The high temperature peak (around 375K) observed in the sample with the highest fluence was not investigated due to the cryostat thermal limitations.

All observed traps are referred to as E1 and E2 in the following text. Activation energies of electron emission for the E1 and E2 traps have been determined from Arrhenius plots of T 2–corrected electron emission rates (inset in Fig. 3) as follows: E1=(0.48±0.01) eV for the 1×10^{9} cm^{-2}, E1=(0.49±0.03) eV and E2=(0.77±0.03) eV for the 1×10^{10} cm^{-2} and E2=(0.67±0.03) eV for the 2×10^{10} cm^{-2}. All traps appear in concentrations from 1 up to 3×10^{12} cm^{-3}, as determined from the DLTS measurements.

The observed traps E1 and E2 resemble those already reported in the literature, the S_1 [26, 27] defect, and the so-called $Z_{1/2}$ [28, 29], respectively. It should be noted that in the case of the fluence 1×10^{10} cm^{-2} the estimated value for the activation energy is a little bit higher than the reported values, but this is due to the fact that the E1 and E2 traps are closely spaced, and the low temperature E1 peak (so called "shoulder") overlaps with the E2 peak, which leads to the certain errors in energy estimation. However, the situation clears out for the sample irradiated with 2×10^{10} cm^{-2}, where without interference of the low temperature peak we have been able to correctly estimate the energy of the E2 trap.

The S_1 is usually observed after electron irradiation or ion implantation. Its origin is still not very clear, but it has been assigned to the interstitial carbon [26]. However, a recent study suggests a much more complex structure of this defect [30]. This is in a good agreement with our results, and the observed, significant, change in the doping level.

The $Z_{1/2}$ defect is one of the most studied defects in SiC. It is an intrinsic, carbon-related defect. It is an acceptor like defect with an extreme thermal stability up to 2000 °C [27]. It has been shown that $Z_{1/2}$ defect limits the minority carrier lifetime and therefore strongly affects device properties [31]. Very recently the microstructure of $Z_{1/2}$ was revealed to be a single carbon-vacancy [32, 33].

C. CCE deterioration in selectively irradiated 4H-SiC SBD

The charge collection efficiency as a function of the irradiation fluence for both 4 and 2 MeV He irradiations are shown in figures 4 and 5 respectively. The figures summarize the results for all the probe ion beams used (1, 2, 3, 4 and 6 MeV He) as well as different bias voltages (sections a, b and d of figures 4 and 5). For comparison the SRIM simulated ionization depth profiles of PIBs and the vacancy-recoil depth profile of DIB, as well as the calculated extent of the depletion region for given bias, are shown in Figures c for both irradiation energies. Their interplay is essential for understanding the charge collection mechanism and for the interpretation of the experimental CCE data [4]. The CCE decreases for different (PIB, DIB, BIAS) settings at different rates similar to previous observations in silicon diodes [3]. In contrast to silicon diodes irradiated with even higher He fluences, CCE distributions for 4H-SiC SBD can't be simulated by the linear model [4] over the entire DIB fluence range (1×10^{9} – 5×10^{11} cm^{-2}), even for the highest applied bias voltage of -400 V associated with a complete generation of free carriers within a depleted region and pure drift motion of carriers towards collecting electrodes. Above a fluence of 1×10^{11} cm^{-2} significant

deviations from linear dependence occur for some of studied cases.

For a moment we will restrict our discussion to the linear behavior of CCE decrease. Within the 1×10^{9} – 1×10^{11} cm^{-2} fluence range, particularly for -400 and -200 V bias settings, the CCE decrease can be approximated by a linear dependence (inset graphs in Fig.4 and Fig.5 for partly damaged 4H-SiC SBD with 4 MeV He and 2 MeV He respectively. In following we discuss the decrease of CCE for both irradiation energies, taking into account i) the previous observation from DLTS measurements that electron traps are created in the ion implanted region of 4H-SiC SBD (3.B) and ii) the fact that free electrons are moving from the negatively biased Schottky contact towards the grounded back Ohmic contact, while holes are moving in the opposite direction:

1. When the probe range is small compared to both the damaged layer depth and the depletion depth (PIB=1, 2, 3 MeV He and DIB=4 MeV He), the highest CCE values are observed, very close to the perfect value of one (1) up to fluence value of 10^{11} cm^{-2}. Only a part of free electrons drifting through damaged region is being trapped and don't contribute, whereas all created holes contribute to the induced charge. The hole contribution to induced charge is small due to a short drift distance. The electron contribution dominates, even in a case of partial electron trapping.
2. In the same case of deep damage created by 4 MeV He, the measured CCE value decreases as a PIB is penetrating closer to the damaged layer, because the average drift distance of later captured electrons decreases for more penetrating particles, but this is only distinguishable for fluences of $10^{11}cm^{-2}$ and larger, where electron trapping becomes more pronounced.
3. In the case of relatively shallow damage created by 2 MeV He, the highest CCE value is recorded for the deepest penetrating particle (PIB=6 MeV He) at bias of -400 V. Only a small fraction of the created electrons has to drift through the damaged layer, whereas all other charge carriers are collected. But those electrons created at a depth above the damaged layer, contribute to the induced charge the most (the largest average drift distance if not trapped). So when the trapping probability of those electrons increases for larger fluence values, the CCE measured by a very deep probe decreases to the lowest values.
4. In the 2 MeV He irradiation case when a probe ionization maximum is just below the shallow damaged layer (PIB=3 MeV He and DIB=2 MeV He, green symbols), high values of CCE are measured across the whole fluence range because in that particular

studied case i) the majority of created free electrons are insensitive to the damage and ii) the electron contribution dominates over the hole contribution.

5. When the PIB range is equal to the DIB range (orange for 4 MeV and cyan symbols for 2 MeV He) the CCE decrease is larger compared to lower probe energies, because a large portion of free electrons originating from the damaged layer can be immediately trapped. The CCE decrease becomes more pronounced for fluence values above 10^{11} cm^{-2} corresponding to a larger trapping probability.
6. The lowest CCE values for bias voltage of -400 V in a case of deep damage (4 MeV He) are recorded when a probe has an even larger end of range (PIB=6 MeV and DIB=4 MeV He, red symbols). Both electrons and holes (which are created either in the region closer to the surface or beyond the damaged region respectively) have to traverse through this damaged region where majority of electrically active $Z_{1/2}$ traps are formed by DIB. The electron mobility in the low doped 4H-SiC (μ_n=950 $cm^2V^{-1}s^{-1}$) [34] is much larger than the hole mobility (μ_p=115 $cm^2V^{-1}s^{-1}$). The same trap that captures a fast drifting electron and becomes negatively charged might capture a later arriving slow moving hole. Moreover, the electrons created beyond the damaged layer are insensitive to formed traps, but their average drift distance and contribution to induced charge is relatively small.
7. Additionally, in a case of a deep probe some carriers are generated beyond the extent of depleted region at reverse biases of -100 V and -200 V. Their motion is governed by diffusion until they reach the edge of depleted region. Only minority carriers (holes) contribute to the induced charge. The contribution from electrons generated in that field free (and defect free) region is lost. Corresponding CCE distributions (PIB=6 MeV He, BIAS= -100 & -200 V; red symbols) show opposite curvature (towards higher values) from initial linear dependence and are not considered further here.

Figure 6 shows selected IBIC spectra for 4 MeV and 2 MeV irradiated samples, figures a-c and d-f respectively. These illustrate the origin of the non-linear behavior manifested as bending towards CCE values lower than estimated by a linear dependence for the two largest fluence values of 2×10^{11} and 5×10^{11} cm^{-2}. These IBIC peaks are extracted from the recorded event by event list files for PIB detection in each partially damaged area of SBD corresponding to particular DIB fluence value. Their position (channel number) corresponds to the measured amplitude of induced charge signal, while their height corresponds to the normalized yield. IBIC peaks are 1) slightly widening (FWHM increases) and 2) slowly moving towards lower channel values (amplitude of recorded IBIC signal decreases). They

further illustrate that up to the fluence value of 1×10^{11} cm^{-2} the shape of IBIC peak does not differ from the initial Gaussian shape extracted from a non-irradiated area of the SBD. But IBIC peaks significantly change their centroid position (amplitude), peak resolution (FWHM) and even shape (deviations from Gaussian distribution) for DIB fluences of 2×10^{11} and 5×10^{11} cm^{-2}. This abrupt change in spectral performance of tested SBDs could be related to: 1) significant decrease of charge carrier lifetime due to increasing $Z_{1/2}$ concentration in damaged region with increasing fluence (3.B), 2) decrease of free carrier concentration with increasing fluence (3.A) and 3) changes of electric field profile within disordered region created by DIB.

Additionally, formation of new type of defects, i.e. complex (cluster) defects within disordered region created by DIB, even for fluence values in the 1×10^{11} cm^{-2} range (not investigated here using the single ion implantation), could have an important role on performance of the tested 4H-SiC SBD. Roccaforte et al. suggested the point defect reorganization/clustering in SiC irradiated with 1 MeV Si ions above the fluence value of 5×10^{9} cm^{-2} [15] and we already proved a direct formation of the small clusters of di-vacancies in n-type CZ silicon (N_{eff}~10^{14} cm^{-3}) with no thermal treatment after the irradiation with 8.3 MeV Si ions to the fluence value of 1×10^{10} cm^{-2} [8].

4. **Conclusions**

We put the detector grade 4H-SiC material to comprehensive radiation hardness test using light He ions in the MeV energy range. The very high CCE values in the 0.95-1.0 range have been obtained using the partially damaged SBD irradiated up to the fluence value of 1×10^{11} cm^{-2}. The CCE decrease is linearly dependent of a fluence in the same range. Above He fluences of 1×10^{11} cm^{-2} a significant deviation from the linear behavior of CCE decrease has been observed in some cases. Previous radiation resistance studies performed on the SBD made from n-type 4H-SiC material with similar N-doping concentration do not mention a deviation from the linear behavior of CCE if irradiated with electrons [6, 12], protons [11, 12] or other light ions [11].

If we restrict ourselves to only a case of the probe being the same as the damaging ion (PIB=DIB=2 MeV He), and take into account only the results obtained for the highest bias of -400 V (Fig.5a, cyan symbols), our measured CCE values as a function of fluence closely match those reported by K.K. Lee et al. [11] and can be simulated by a linear decrease within statistical error.

We also observed a substantial change in the detection performance of partly damaged 4H-

SiC SBD irradiated with He fluence values above 1×10^{11} cm^{-2} even for the highest applied bias voltage.

Results from electrical and DLTS measurements suggest both observed effects could be related to the localized formation of deep defects associated with carbon interstitials (S_1) and carbon vacancies ($Z_{1/2}$) within the ion implantation range.

In comparison, the sudden change in spectroscopy performance and the non-linear behavior of the CCE haven't been observed with the FZ Si detector diodes irradiated up to 1×10^{12} cm^{-2} [35] and the CZ Si diodes irradiated up to 5×10^{11} cm^{-2} [4] of He ions having similar energies. Therefore here presented study supports a hypothesis of the worse radiation hardness of this particular 4H-SiC material for the MeV light (He) ion detection at room temperature in comparison to extensively studied low doped detector grade silicon materials.

5. **Acknowledgement**

The authors wish to acknowledge the support of the ANSTO Accelerator Science Project No.0208 and the IAEA under the CRP project #F11016.

6. **References**

[1] E. Chason, S. T. Picraux, J. M. Poate, J. O. Borland, M. I. Current, T. Diaz de la Rubia, D. J. Eaglesham, O. W. Holland, M. E. Law, C. W. Magee, J. W. Mayer, J. Melngailis, and A. F. Tasch, J. Appl. Phys. **81**, 6513 (1997).

[2] L. Pelaz, L.A. Marques, M. Aboy, P. Lopez and I. Santos, Eur. Phys. J. B **72**, 323 (2009).

[3] Z. Pastuovic, M. Jaksic, G. Kalinka, M. Novak, A. Simon, IEEE Trans. Nucl. Sci. **56**, 2457 (2009).

[4] Z. Pastuovic, E. Vittone, I. Capan, M. Jaksic, Appl. Phys. Lett. **98**, 092101 (2011).

[5] I. Zamboni, Z. Pastuovic, and M. Jaksic, Diam. Relat. Mater. **31**, 65 (2013).

[6] N. Iwamoto, B.C. Johnson, N. Hoshino, M. Ito, H. Tsuchida, K. Kojima and T. Ohshima, J. Appl. Phys. **113** (2013) 143714.

[7] T. Ohshima, S. Sato, M. Imaizumi, T. Nakamura, T. Sugaya, K. Matsubara, S. Niki, Solar Energy Materials & Solar Cells **108**, 263-268 (2013).

[8] Z. Pastuovic, I. Capan, R. Siegele, R. Jacimovic, J. Forneris, D.D. Cohen and E. Vittone, Nucl. Instr. Meth. Phys. Res. B **332**, 298 (2014).

[9] C. Leroy and P.G. Ranciota, Rep.Prog. Phys. **70**, 493 (2007).

[10] N. Dharmarasu, M. Yamaguchi, J.C. Bourgoin, T. Takamoto, T. Ohshima, H. Itoh, M. Imaizumi and S. Matsuda, Appl. Phys. Lett. **81**(1), 64 (2002).

[11] K.K. Lee, T. Ohshima, A. Saint, T. Kamiya, D.N. Jamieson, H. Itoh, Nucl. Instr. Meth. Phys. Res. B 210, 489 (2003).

[12] F. Nava, E. Vittone, P. Vanni, G. Verzellesi, P.G. Fuochi, C. Lanzierif, M. Glaser, NIM A **505**, 645 (2003).

[13] A. Castaldini, A. Cavallini, L. Rigutti, F. Nava, S. Ferrero and F. Giorgis, J. Appl. Phys. **98**, 053706 (2005).

[14] F. Nava, A. Castaldini, A. Cavallini, P. Errani and V. Cindro, IEEE Trans. Nucl. Sci. **53** (5), 2977 (2006).

[15] F. Roccaforte, S. Libertino, V. Ranieri, A. Ruggiero, V. Massimino and L. Calcagno, J. Appl. Phys. **99**, 013515 (2006).

[16] N. B. Strokan, A.M. Ivanov and A.A. Lebedev, Nucl. Instr. Meth. Phys. Res. A **569**, 758 (2006).

[17] T. Moore, EPRI J. **22**, 30 (1997).

[18] W. Wondrak, R. Held, E. Niemann, and U. Schmid, IEEE Trans. Ind. Electron. **48**, 307 (2001).

[19] D. M. Brown, E. Downey, M. Ghezzo, J. Kretchmer, V. Krishnamurthy, W. Hennessy, and G. Michon, Solid-State Electron. **39**, 1541 (1996).

[20] A. Itoh and H. Matsunami, Phys. Stat. Sol. A **162**, 389 (1997).

[21] S.-H. Ryu, A. K. Agarwal, R. Singh, and J. W. Palmour, IEEE Electron Device Lett. **22**, 127 (2001).

[22] M. Ito, L. Storasta, and H. Tsuchida, Appl. Phys. Express. **1**, 015001(3) (2008).

[23] E. Vittone, ISRN Material Science Vol.2013, Article ID 637608.

[24] R. Siegele, A.G. Kachenko, M. Ionescu, D.D. Cohen, Nucl. Instr. Meth. B **267**, 2054 (2009).

[25] Available at: <http://www.srim.org>.

[26] M. L. David, G. Alfieri, E. V. Monakhov, A. Hallén, C. Blanchard, B. G. Svensson, and J. F. Barbot, J.Appl. Phys. **95**, 4728 (2004).

[27] G. Alfieri, E. V. Monakhov, B. G. Svensson, M. K. Linnarsson, J. Appl. Phys. **98**, 43518 (2005).

[28] C. Hemmingsson, N. T. Son, O. Kordina, J. P. Bergman, E. Janzén, J. L. Lindström, S. Savage and N. Nordell, J. Appl. Phys. **81**, 6155 (1997).

[29] T. Dalibor, G. Pensl, T. Kimoto, H. Matsunami, S. Sridhara, R. P. Devaty and W.J. Choyke, Diamond Relat. Mater. **6**, 1333 (1997).

[30] L. S. Løvlie, L. Vines and B. G. Svensson, J. Appl. Phys. **111**, 103719 (2012).

[31] L. S. Løvlie and B. G. Svensson, Appl. Phys. Lett. **98**, 052108 (2011).

[32] N. T. Son et al., Phys. Rev. Lett. **109** 187603 (2012).

[33] K. Kawahara et al., J. Appl. Phys. **115** 143705 (2014).

[34] M. Roschke and F. Schwartz, IEEE Trans. Nucl. Sci. Vol. **48**, No. **7**, 1442 (2001).

[35] E. Vittone. IAEA CRP #11016, Technical Report V: „CCE degradation of the n-type diode N#26 from Helsinki Institute of Physics“

Table 1

Details about irradiation conditions (type, area, ion microbeam energy, ion rate, pixel dwell time, and time required for irradiation) used to create partial damage in chosen 4H-SiC SBDs.

Sample	Irradiation	Area [μm^2]	E(He^{2+}) [MeV]	Fluence [cm^{-2}]	µbeam rate [kcps]	Pix. dwell time [µs]	Irrad. time [min]	Analysis
#1	Patterned	100×100 (9)	4	$10^9 – 5×10^{11}$	1, 2, 5, 10	500, 1000	0.5 – 21	IBIC
#2	Patterned	100×100 (9)	2	$10^9 – 5×10^{11}$	1, 2, 5, 10	500, 1000	0.5 – 21	IBIC
#3	Homogenous	1000×1000	2	10^9	5	1000	33	C-V, DLTS
#8	Homogenous	1000×1000	2	$5×10^9$	10	500	83	C-V
#4	Homogenous	1000×1000	2	10^{10}	10	500	166	C-V, DLTS
#12	Homogenous	1000×1000	2	$2×10^{10}$	10	500	333	C-V, DLTS

Figure captions

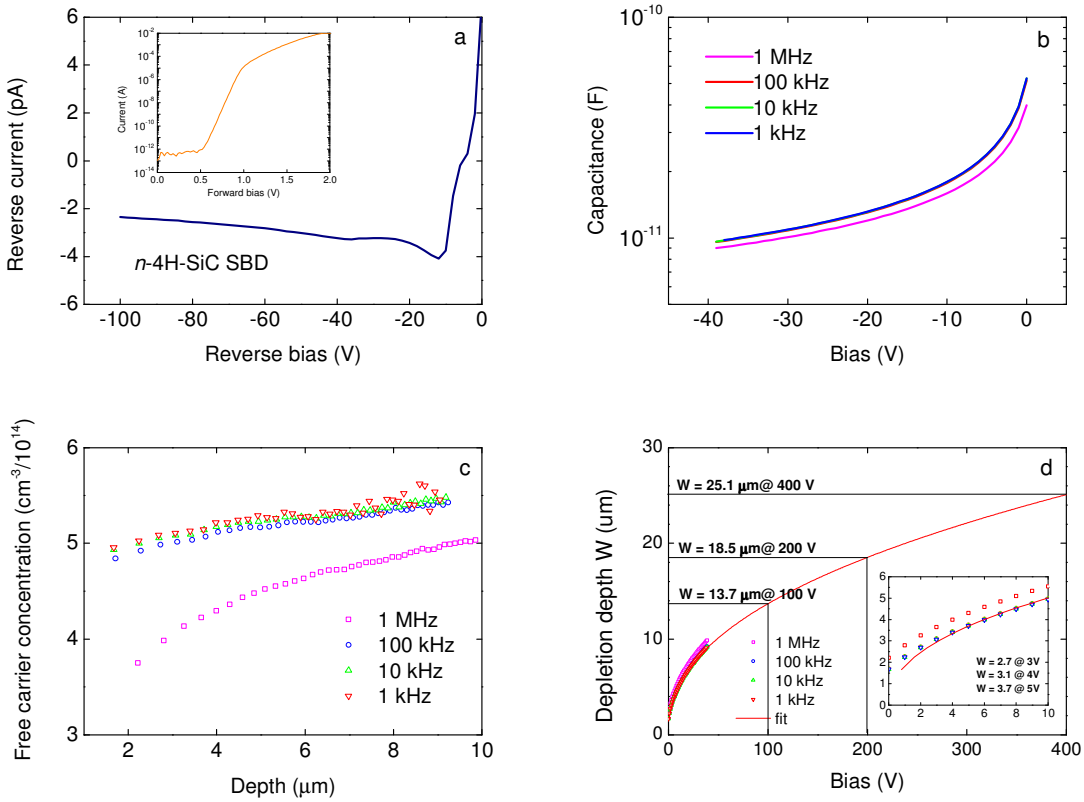

Fig.1 Measured and calculated electrical properties of the as prepared non-irradiated 4H-SiC SBD: (a) the reversed current (inset in Fig. 1(a) shows forward current), (b) C-V characteristic, (c) free carrier concentration depth profile and (d) bias dependence of the depletion depth.

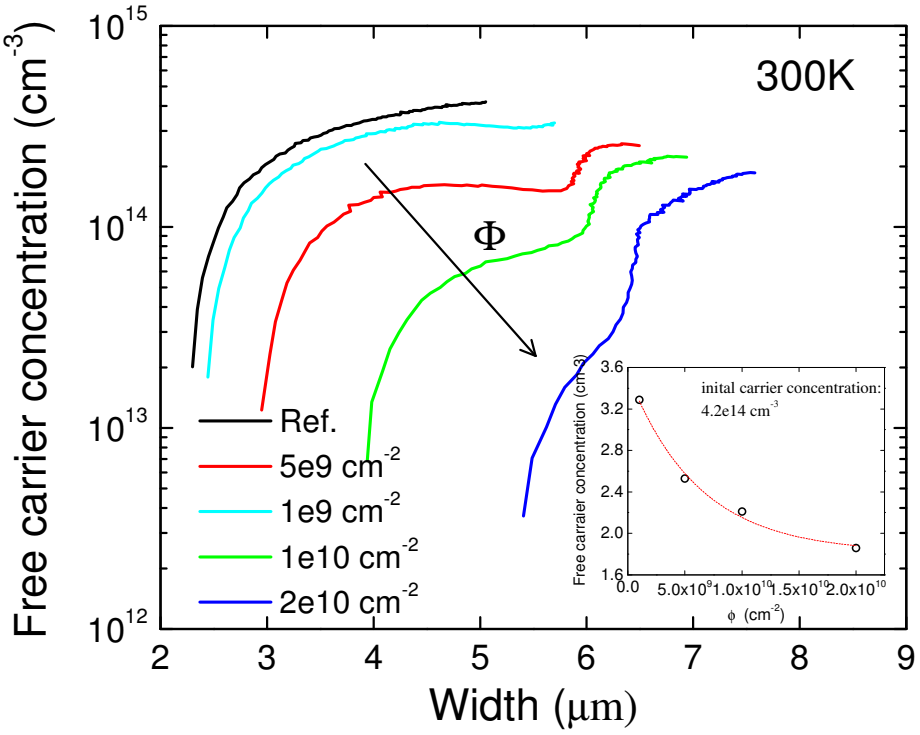

Fig.2 Free carrier concentration depth profiles obtained for different fluence values used to homogenously irradiate the 4H-SiC samples with raster scanned 2 MeV He ion microbeam. Inset shows the free carrier concentration decrease as a function of accumulated ion fluence as deduced from the C-V measurements.

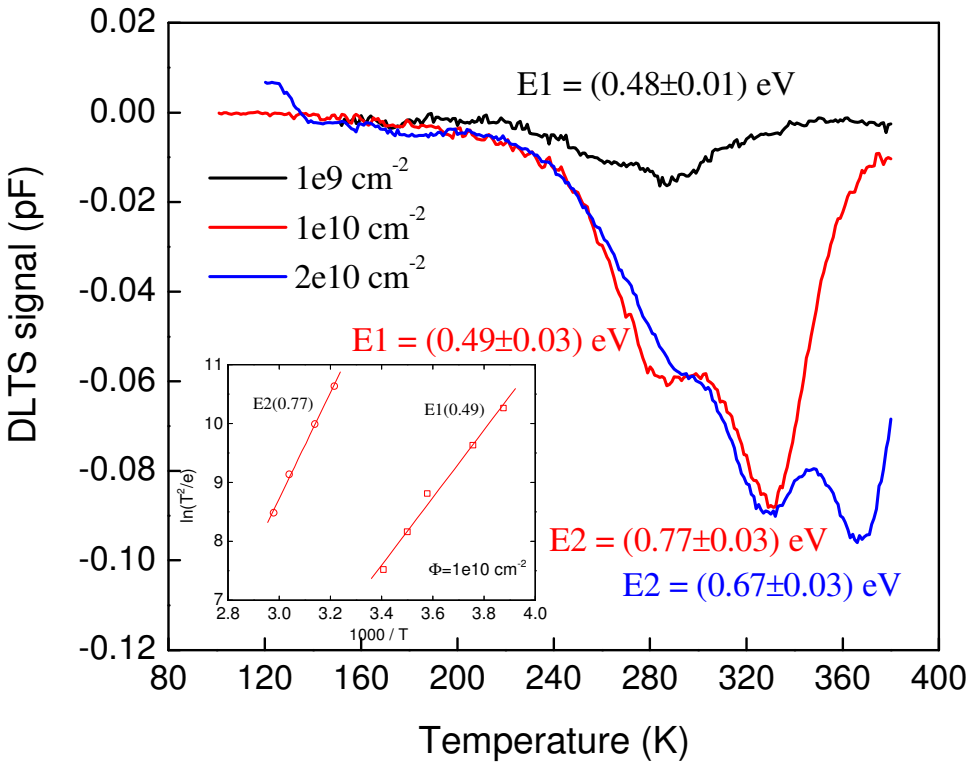

Fig.3 Results of DLTS spectroscopy performed on 4H-SiC Schottky barrier diodes implanted by 2.0 MeV He single ions using raster scanned microbeam. Normalized DLTS spectra measured at reverse bias -4 V and the rate window of 50ms are shown for samples irradiated up to fluence values of 1×10^{9} cm^{-2} (black), 1×10^{10} cm^{-2} (red) and 2×10^{10} cm^{-2} (blue). Inset in Fig.2 shows the Arrhenius plots of T 2–corrected electron emission rates for the sample irradiated up to 1×10^{10} cm^{-2}. Determined activation energies of electron emission for the identified E1 and E2 traps are shown next to corresponding peaks in DLTS spectra.

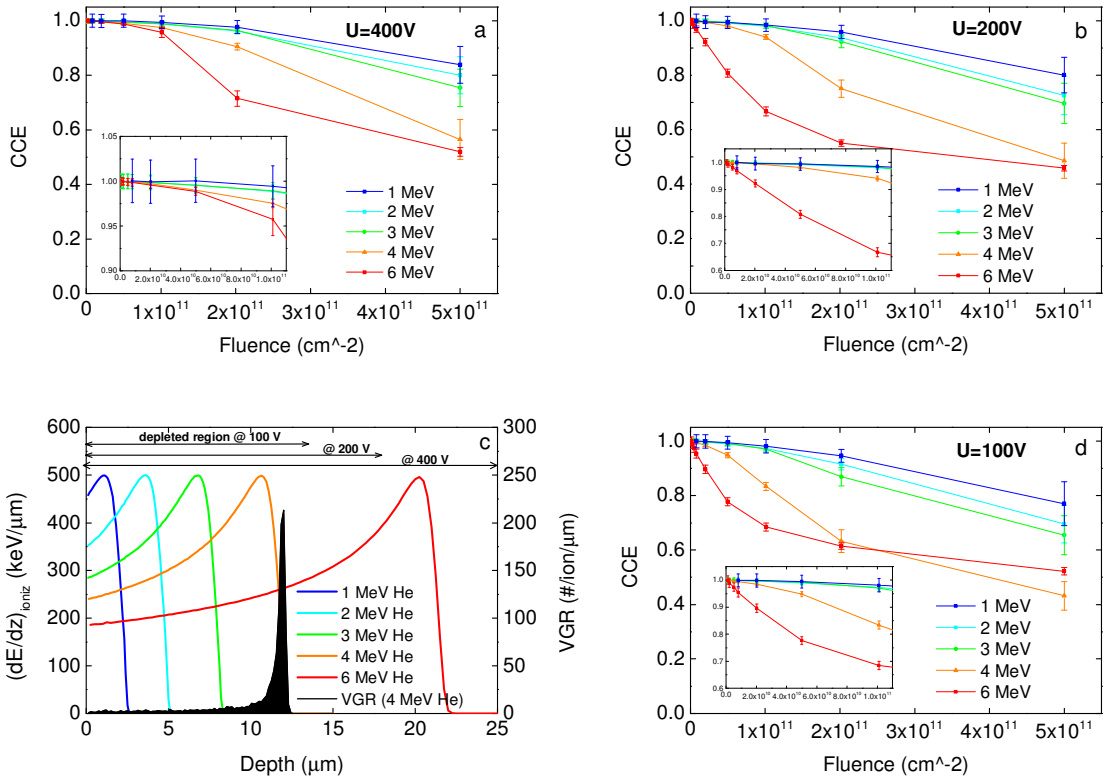

Fig.4 Calculated CCE values measured in IBIC experiments using 1,2,3,4, and 6 MeV He ions (PIB) on the 4H-SiC SBD irradiated selectively with increasing fluences of 4 MeV He ions (DIB). Results are shown for the partly damaged 4H-SiC SBD reversely biased at -400 V (a), -200 V (b) and -100 V (d). Fig.4(c) shows the ionization depth profiles of used PIBs, vacancy-recoil depth profile of DIB (black) and extent of the depletion region for applied biases (arrows). The lines connecting the data points are reported to guide the eye only.

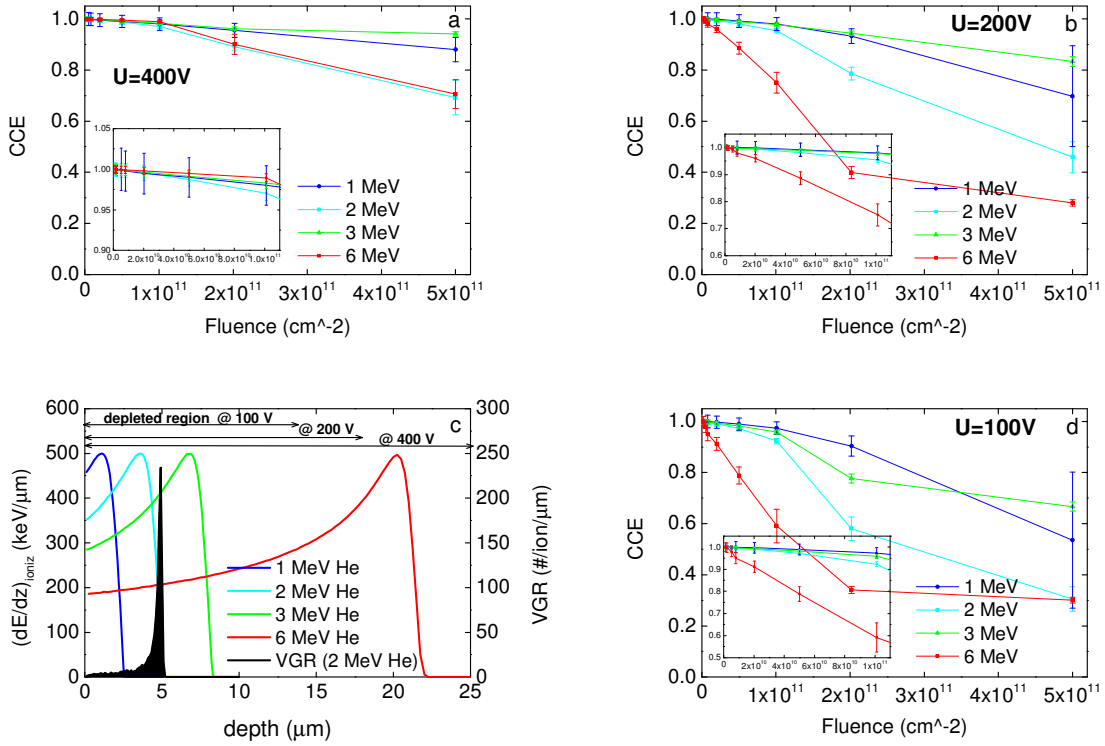

Fig.5 Calculated CCE values measured in IBIC experiments using 1, 2, 3, and 6 MeV He ions (PIB) on the 4H-SiC SBD irradiated selectively with increasing fluences of 2 MeV He ions (DIB). Results are shown for the partly damaged 4H-SiC SBD reversely biased at -400 V (a), -200 V (b) and -100 V (d). Fig.5(c) shows the ionization depth profiles of used PIBs, vacancy-recoil depth profile of DIB (black) and extent of the depletion region for applied biases (arrows). The lines connecting the data points are reported to guide the eye only.

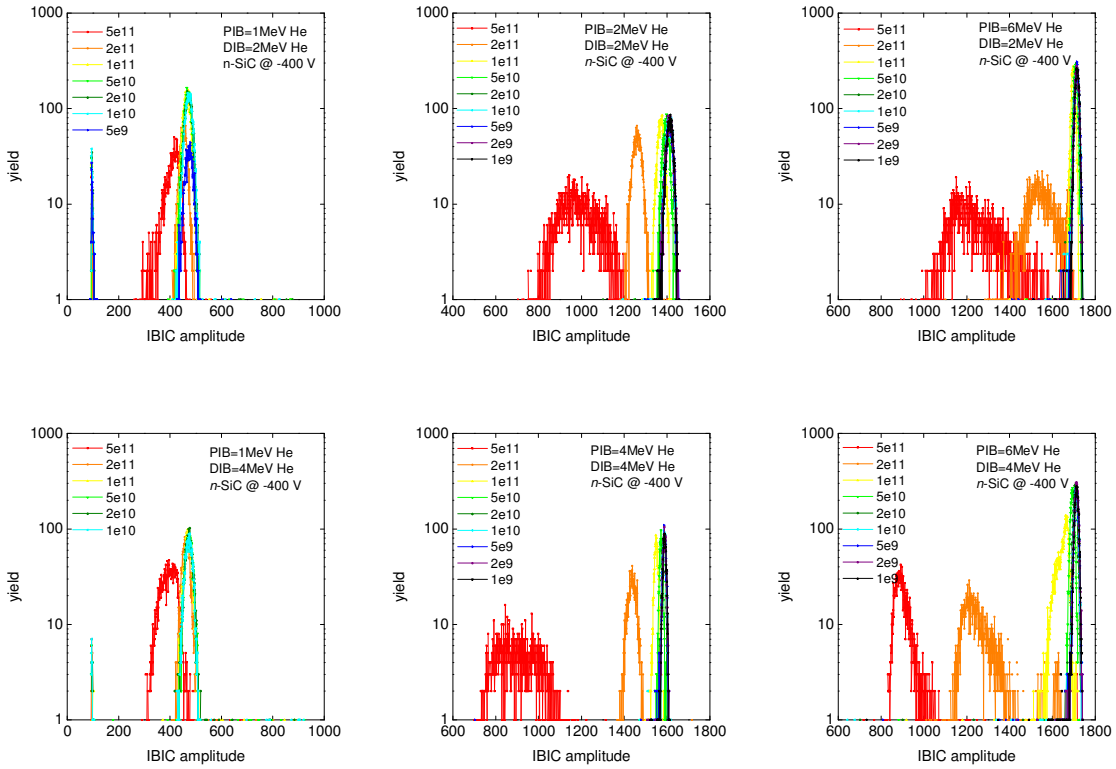

Fig.6 Off –line extracted IBIC spectra showing the detection performance of selected probing ions (PIB) by two partly damaged 4H-SiC SBDs biased at -400 V: selectively irradiated by 2 MeV He (a-c) and 4 MeV He ion microbeam (d-f).